

Chapter 2

Modelling, Performance Optimisation and Automated Design of Mixed-Technology Energy Harvester Systems

Tom J. Kaźmierski and Leran Wang

Abstract This chapter presents an automated energy harvester design flow which is based on a single HDL software platform that can be used to model, simulate, configure and optimise the complete mixed physical-domain energy harvester system (micro-generator, voltage booster, storage element and load). We developed an accurate HDL model for the energy harvester and demonstrated its accuracy by validating it experimentally and comparing it with recently reported models. A demonstrator prototype incorporating an electromagnetic mechanical-vibration-based micro-generator and a limited number of library models has been developed and a design case study has been carried out. Experimental measurements have validated the simulation results which show that the outcome from the design flow can improve the energy harvesting efficiency by 75%.

Keywords Kinetic energy harvester · Design flow · Optimisation · Mixed-domain modelling

2.1 Introduction

At present there are considerable and continuing research efforts worldwide to support the energy harvesting paradigm and self-powered electronics. The majority of the reported research in energy harvesting has been on improving the efficiency of the energy harvesters through the design and fabrication of novel micro-generators, materials and devices [3]. The amount of power that can be harvested in a particular application is highly dependent upon the energy source being harvested. Typically, power densities of around $800 \mu\text{W}/\text{cm}^3$ for machine vibration applications and up to $140 \mu\text{W}/\text{cm}^3$ for human-powered applications can be expected [4]; however, the power output of vibration-harvesting inertial generators is highly sensitive to the frequency and amplitude of the vibration source [8] and so these figures are indicative only. Practical generators have been reported with power densities of 17

T.J. Kaźmierski (✉)

School of Electronics and Computer Science, University of Southampton, Southampton, UK
e-mail: tjk@ecs.soton.ac.uk

$\mu\text{W}/\text{cm}^3$ for a non-resonant device [6, 9], to a resonant device capable of generating $30 \mu\text{W}/\text{cm}^3$. Typically the generated voltage from a micro-generator is insufficient to power an electronic device directly, and therefore external analogue circuits are often employed to rectify and boost the voltage and store the energy in a battery or a supercapacitor. Various circuit designs have also been reported, such as an AC/DC rectifier combining with a switch-mode DC/DC converter [11] and self-timed circuits which eliminate AC/DC conversion [15]. Because of the output power of energy harvesters is highly variable and unpredictable, recently Amirtharajah et al. proposed digital circuits that employ serial computation and distributed arithmetic as a way of dealing with the variability of the available energy [1]. Also, in the publication of Wang et al., it was reported through the use of dedicated sub-threshold logic it is possible to implement an FFT processor that operates in practice with supply voltage as low as 180 mV, suitable for energy harvesters [20]. Electrical power management technique has also been investigated. “The charge-based control unit will make sure the energy available is enough for the atomic operation before triggering the computation” [14, 19].

An energy harvester has normally three main components: the micro-generator which converts ambient environment energy into electrical energy, the voltage booster which pumps up and regulates the generated voltage and the storage element (Fig. 2.1).

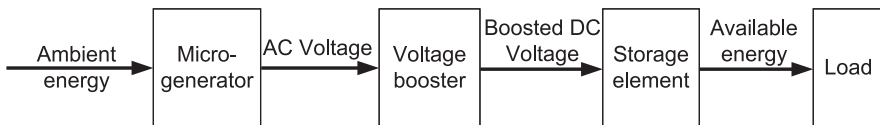


Fig. 2.1 Block diagram of an energy harvester

Clearly such an energy harvester consists of components from both mechanical and electrical domains as well as external circuits which regulate and store the generated energy. Therefore, the performance optimisation should only be based on a model that describes the energy harvester as an integrated system. However, most existing modelling and optimisation methods are concentrating on either the micro-generator [21] or the external circuits [1] separately while the design tools for an integrated system are missing. MATLAB and finite element analysis (FEA) packages are being used to simulate and optimise the performance of the micro-generator part of the self-powered system [2]. To design and optimise the energy harvester associated electronics, simulators such as SPICE are often used. The micro-generator is usually modelled either as an ideal voltage source [22] or an equivalent circuit model [1] because “the current EDA tools do not support direct integration of the electromechanical dynamics of vibration-based energy harvesters into circuit simulations” [1].

To design highly efficient energy harvesters, it is crucial to consider the various parts of an energy harvester in the context of a complete system, or the gain at one part may come at the price of efficiency loss elsewhere, rendering the energy harvester much less efficient than expected. To date there has been no reported design flow for energy harvesters and the aim of this chapter is to propose such an automated

design flow for the modelling, configuration, and optimisation of energy harvester systems through the use of VHDL-AMS. VHDL-AMS can be used to model and correctly predict the performance of an energy harvester system because it describes the micro-generator and external electronics as an integrated model, so that the close mechanical–electrical interaction, which is often missing in traditional energy harvester design methods, can be captured accurately.

2.2 Energy Harvester Design Flow

This chapter proposes an automated energy harvester design flow which is based on a single HDL software platform that can be used to model, simulate, configure and optimise energy harvester systems. The proposed design flow is outlined in the pseudo-code of Algorithm 1 and also shown in Fig. 2.2. Naturally, the process starts with initial design specification, such as available energy source (light, heat, vibration, etc.), environmental energy density, device size, minimum voltage level/power output. According to these specifications, HDL models are constructed from component cells available in the component library. The component library contains parameterised models of different kinds of micro-generator structures (solar cell, electromagnetic, piezoelectric, etc.), various booster circuit topologies and storage elements. The outer loop in the algorithm represents this structure configuration process, which involves examining and comparing those HDL models from the library with the aim of identifying a set of components that meet specific user requirements. The inner design flow loop will then find the best performance of each candidate design by adjusting electrical and non-electrical parameters of the design's mixed-technology HDL model. The parametric optimisation of the generated structure will further improve the energy harvester efficiency by employing suitable optimisation algorithms. The design flow ends at the best performing design for fabrication subject to the user-defined performance characteristics.

Algorithm 1 Automated energy harvester design flow.

```

Initial design structure and specification
Structure configuration loop:
for all design structures do
    Build HDL model of design
    Optimisation loop:
    repeat
        Simulate and evaluate performance
        if best performance not achieved then
            Update design parameters
        end if
    until best performance achieved
    if there are more structures to try then
        Select new structure
    end if
end for

```

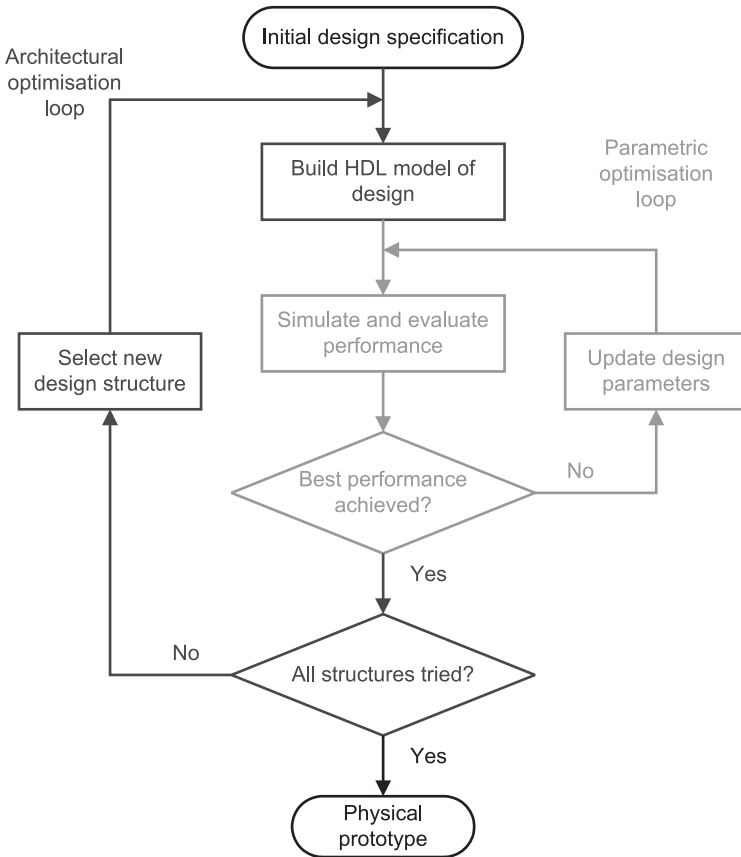


Fig. 2.2 Energy harvester design flow

The requirements for energy harvester component models are: (1) models need to be computationally efficient for fast performance optimisation when used in complete energy harvester systems and yet accurate, these are conflicting requirements; (2) models need to capture both theoretical equations and practical non-idealities required for accurate performance estimation. The models should support different mechanical–electrical structures and will be expressed in terms of HDL descriptions. They will be able to predict the behaviour of the actual device accurately while remaining reconfigurable.

As proof of concept, a small VHDL-AMS model library has been built to demonstrate the efficiency of the design flow, which is shown in Section 2.3. Based on the developed model library, Section 2.4 describes the automated structure configuration that has been carried out using a single VHDL-AMS simulator. The configuration result and simulations of different energy harvester models have led to in-depth understanding about how electromagnetic micro-generator performs when

connected with voltage multipliers. The results have been used for the performance optimisation, which is presented in Section 2.5.

2.3 Energy Harvester Modelling

2.3.1 Micro-generator

Reported modelling approaches aim to replace the micro-generator of an energy harvester with either an ideal voltage source (Fig. 2.3a) [22] or an equivalent circuit model (Fig. 2.3b) [1] when designing the voltage booster. However, as will be shown later, neither of these approaches is suitable for accurate voltage booster design.

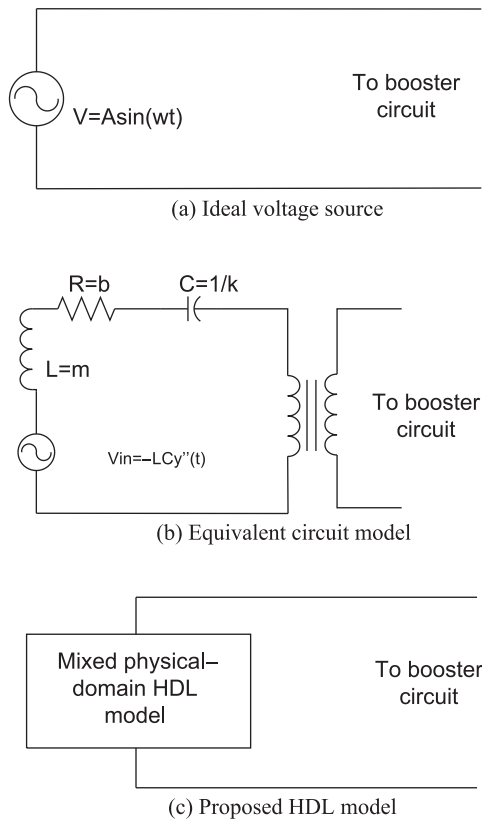


Fig. 2.3 Micro-generator models

The proposed approach uses VHDL-AMS to describe the micro-generator as a series of analytical equations (Fig. 2.3c), which includes mechanical, magnetic and electrical behaviours of the micro-generator. Throughout this section, comparisons

have been made between different modelling approaches and it has been demonstrated that the proposed HDL-based model is more accurate than the circuit models.

The case study presented here uses a vibration-based electromagnetic micro-generator which was developed by Torah et al. [16] as an example. The design is based on a cantilever structure. The coil is fixed to the base and four magnets, which are located on both sides of the coil, form the proof mass (see Fig. 2.4).

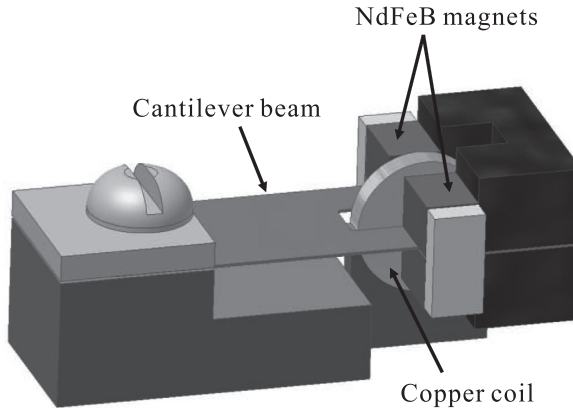


Fig. 2.4 Cantilever-based electromagnetic micro-generator [16]

This structure can be modelled as a second-order spring-damping system, which has been widely used, and whose dynamics is [3]

$$mz''(t) + c_p \dot{z}(t) + k_s z(t) + F_{em} = -m\ddot{y}(t) \quad (2.1)$$

where m is the proof mass, $z(t)$ is the relative displacement between the mass and the base, c_p is the parasitic damping factor, k_s is the spring stiffness, $y(t)$ is the displacement of the base and F_{em} is the electromagnetic force.

The electromagnetic voltage generated in the coil is given by Faraday's law:

$$v_{em} = \Phi(z) * \dot{z}(t) \quad (2.2)$$

where $\Phi(z)$ is the magnetic flux through the coil.

Although the developed HDL model is based on analytical equations, it can capture practical size and shape of the actual device. The coil in the actual micro-generator consists of N turns and has an inner diameter r and outer diameter R . Each of the four opposite magnets are of height H (see Fig. 2.5a).

So the actual magnetic flux through the coil is a piecewise non-linear function of the relative displacement $z(t)$: $\Phi = f\{z(t)\}$.

When the relative displacement is small $|z(t)| < r$ (Fig. 2.5b):

$$\Phi = \left(\sqrt{R^2 - z^2(t)} + \sqrt{r^2 - z^2(t)} \right) * 2 * B * N \quad (2.3)$$

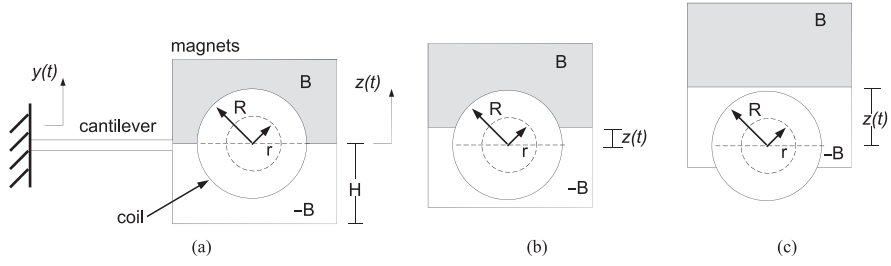


Fig. 2.5 Relative displacement between the coil and magnets in the micro-generator: **(a)** initial position $z(t) = 0$; **(b)** small displacement $|z(t)| < r$; and **(c)** large displacement $H - r < |z(t)| < H$

When the relative displacement is large $H - r < |z(t)| < H$ (Fig. 2.5c):

$$\Phi = - \left(\sqrt{R^2 - (H - |z(t)|)^2} + \sqrt{r^2 - (H - |z(t)|)^2} \right) * B * N \quad (2.4)$$

There are five other sections of the piecewise function which have been implemented in the VHDL-AMS model (see the code on page 80) but are omitted here.

The output voltage is simply defined by Kirchoff's voltage law:

$$v(t) = v_{em} - R_c * i(t) - L_c * \dot{i}(t) \quad (2.5)$$

where R_c and L_c are the resistance and inductance of the coil, respectively, and $i(t)$ is the current through the coil.

Finally, the electromagnetic force is calculated as (Lorentz force law):

$$F_{em} = \Phi(z) * i(t) \quad (2.6)$$

In the above equations, the coil parameters are given in number of turns N and resistance R_c . However, when manufacturing a coil, the specification is often given by the thickness t , inner radius r , outer radius R and wire diameter d . To build parameterised HDL models, the relations between these parameters are incorporated and listed below. These equations can be deduced using basic geometry and physics knowledge.

The total wire length is

$$l = \frac{4 * f * t * (R^2 - r^2)}{d^2} \quad (2.7)$$

where f is the fill factor.

The number of turns is

$$N = \frac{l}{2 * \pi * R_{ave}} \quad (2.8)$$

where $R_{\text{ave}} = (R - r)/2 + r$ is the average radius.

The coil resistance is given by

$$R_c = \frac{4 * \rho * l}{\pi * d^2} \quad (2.9)$$

where ρ is the resistivity of the material.

The VHDL-AMS code of the model is given below:

```
library IEEE;
use IEEE.ENERGY_SYSTEMS.all;
use IEEE.MECHANICAL_SYSTEMS.all;
use IEEE.ELECTRICAL_SYSTEMS.all;
use IEEE.math_real.all;
use work.EnergyHarvester.all;

entity EMH is
  port (terminal HOUSE:translational;
        terminal LOAD:electrical);
end entity EMH;

architecture Behaviour of EMH is
  quantity yt across HOUSE to translational_ref;
  quantity zt:DISPLACEMENT;
  quantity emv:VOLTAGE;
  quantity vt across it through LOAD to electrical_ref;
  quantity Fem,abszt,Pout,Phi:real;

begin
  mp*zt'DOT'DOT+Cp*zt'DOT+Ks*zt+Fem== -mp*yt'DOT'DOT;
  Phi*zt'DOT==emv;
  emv==vt-Rc*it-Lc*it'DOT;
  Fem== -Phi*it;
  Pout== -it*vt;
  abszt==abs(zt);
  if 0.0<=abszt and abszt<Rin use
    Phi==(sqrt(abs(Rout**2-zt**2))+sqrt(abs(Rin**2-zt**2)))*2.0*B*N;

  elsif Rin<=abszt and abszt<(Htm-Rout) use
    Phi==sqrt(abs(Rout**2-zt**2))*2.0*B*N*(Rout-abszt)/Rw;

  elsif (Htm-Rout)<=abszt and abszt<Rout use
    Phi==sqrt(abs(Rout**2-zt**2))*B*N*(Rout-abszt)/Rw+
    (sqrt(abs(Rout**2-zt**2))-sqrt(abs(Rout**2-(Htm-abszt)**2)))*B*N*
    (Rout-Htm+abszt)/Rw;

  elsif Rout<=abszt and abszt<(Htm-Rin) use
    Phi== -sqrt(abs(Rout**2-(Htm-abszt)**2))*B*N*(Rout-Htm+abszt)/Rw;

  elsif (Htm-Rin)<=abszt and abszt<Htm use
    Phi== - (sqrt(abs(Rout**2-(Htm-abszt)**2))
    +sqrt(abs(Rin**2-(Htm-abszt)**2)))*B*N;

  elsif Htm<=abszt and abszt<(Htm+Rin) use
    Phi== - (sqrt(abs(Rout**2-(abszt-Htm)**2))+
    sqrt(abs(Rin**2-(abszt-Htm)**2)))*B*N;
```



```

elseif (Htm+Rin)<=abszt and abszt<(Htm+Rout) use
Phi==sqrt(abs(Rout**2-(abszt-Htm)**2))*B*N*(Rout-abszt+Htm)/Rw;
else
Phi==0.0;
end use;
end architecture Behaviour;

```

It has been proved that the maximum average power P_{avelec} that can be delivered to the electrical domain is given by [2]

$$P_{\text{avelec}} = \frac{m^2 * Y^2 * \omega_n^4}{8 * c_p} \quad (2.10)$$

where Y is the amplitude of external kinetic excitation, $\omega_n = \sqrt{k_s/m}$ is the system's resonant frequency. Note that all the simulation and experimental tests in this chapter are based on a 50 Hz sine wave excitation with an amplitude of $Y = 8.4 \mu\text{m}$.

This happens when the system's parasitic damping equals to the electromagnetic damping; therefore, if a load resistance R_l is connected to the micro-generator, its optimal value is [13]

$$R_{\text{loptimal}} = \Phi^2/c_p - R_c \quad (2.11)$$

Two types of this micro-generator have been modelled, which are based on the same structure but have different dimensions. Some of the key parameters are listed in Table 2.1. As can be seen from the table, micro-generator type II is bigger than type I and because the coil is changeable, both the micro-generators can have different wire diameters.

Table 2.1 Micro-generators' parameters

	Type I	Type II
Proof mass m (g)	0.6	2.4
Magnet height H (mm)	2.0	3.0
Field strength B (T)	0.5	0.7
Wire diameter d (μm)	12/16/25	16/25
Coil outer radius R (mm)	1.2	2.45
Coil thickness t (mm)	0.48	1.3

2.3.2 Voltage Booster

Voltage boosters are external circuits to the micro-generator that are used to boost up the output voltage and to perform necessary AC–DC rectification. There are a number of circuit topologies that can be used as a voltage booster. VHDL-AMS has also been used to describe the circuit behaviour by DAEs.

2.3.2.1 Voltage Multiplier

A voltage multiplier (VM), which uses cascaded diodes and capacitors to achieve higher DC voltage from an AC input, meets the requirements of a booster and has been investigated here. There are two types of voltage multiplier based on different configurations, namely Villard (Fig. 2.6a–d) and Dickson (Fig. 2.6e–h) [22]. In the model library, these VMs are configured as 3, 4, 5 and 6 stages.

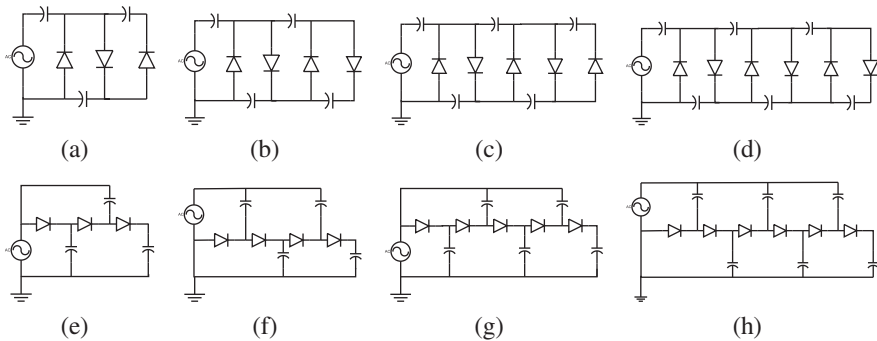


Fig. 2.6 Voltage multiplier configurations, **a–d**: three- to six-stage Villard VM, **e–h**: three- to six-stage Dickson VM

2.3.2.2 Voltage Transformer

A voltage transformer together with a full wave rectifier can also act as the voltage booster for an energy harvester. Two types of rectifier configurations have been tested. Simulation results show that comparing to a common full-bridge rectifier, the configuration in Fig. 2.7 gives better performance since it uses less diodes and thus loses less energy. The number of turns and the resistance value of primary ($N1$, $R1$) and secondary winding ($N2$, $R2$) are the four main parameters that determine the voltage transformer's performance.

2.3.3 Supercapacitor

In case of the storage element, a supercapacitor has been modelled as in Fig. 2.8 [10], where R_{leakage} represents the leakage resistance and R_{ESR} is the equivalent series resistance.

2.3.4 Models Comparison

This section compares the accuracy of different micro-generator modelling approaches with the same voltage booster. Type I micro-generator is connected to

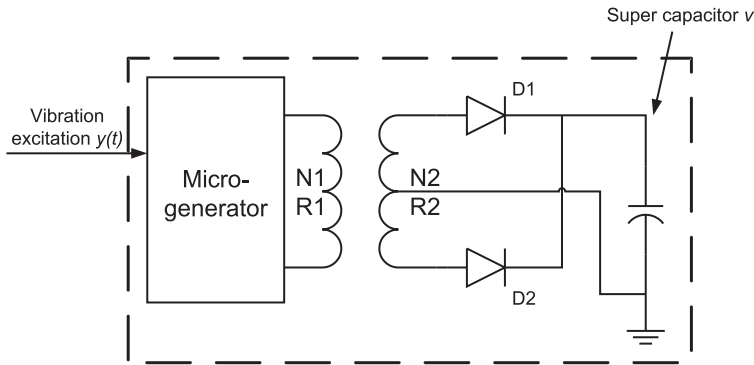


Fig. 2.7 Voltage transformer configuration

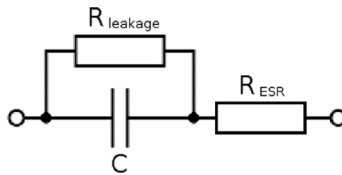


Fig. 2.8 Simplified supercapacitor model

a six-stage Villard voltage multiplier (Fig. 2.6d) and three models of this energy harvester system have been built.

It has been reported that when excited by a 50 Hz sine wave vibration of $8.4 \mu\text{m}$ amplitude, type I micro-generator can generate a maximum power of $45.7 \mu\text{W}$ under the optimal load condition and the output voltage is around 600 mV [16]. So an ideal voltage source (Fig. 2.3a) of 50 Hz frequency and 640 mV amplitude is connected to the VM circuit and SPICE circuit simulations have been carried out to evaluate the VM's performance.

The equivalent circuit model (Fig. 2.3b) of the micro-generator links mechanical mass (m), spring (k) and damper (b) to electrical inductor (L), capacitor (C) and resistor (R) by [1]

$$L = m, \quad C = 1/k, \quad R = b \quad (2.12)$$

and SPICE circuit simulations have also been carried out.

The VHDL-AMS model incorporates the micro-generator and the VM circuit booster.

The comparisons presented in this section are based on the charging of a 0.22 F supercapacitor. Because the VHDL-AMS simulator used here, SystemVision from Mentor Graphics [5], has a maximum simulation time of 150 min, only simulation results in this range have been obtained. Figure 2.9 shows the simulated charging waveform of the capacitor using different micro-generator models including the proposed HDL model. Also shown is the capacitor charging waveform obtained

experimentally. The experiment was set up as the micro-generator sitting on a vibration generator, which produces constant mechanical vibrations (Fig. 2.10a), and the data are collected by LabView software (Fig. 2.10b).

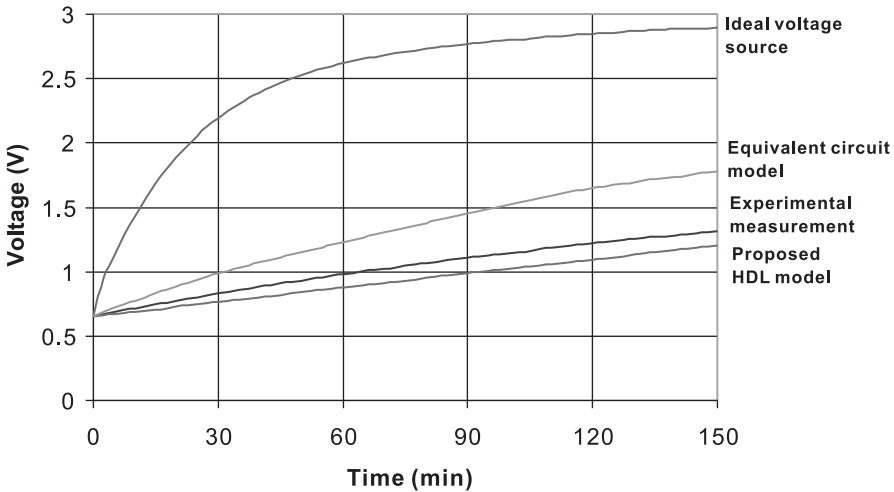


Fig. 2.9 Different energy harvester models compared with experimental measurements

As it can be seen, there is poor correlation between the energy harvester experimental measurements and that of models based on ideal voltage source or equivalent circuit. The reason why the model with ideal voltage source (Fig. 2.3a) fails is that in an energy harvester the voltage booster can greatly affect the behaviour of the micro-generator but an ideal voltage source always produces constant output. The crucial mechanical–electrical interaction is missing in the model.

As for the equivalent circuit model (Fig. 2.3b), this is because Eq. (2.12) is an over-simplification and does not capture accurately the internal operation of the energy harvester.

In the case of the proposed energy harvester HDL model, there is a good correlation between the experimental and simulation results. The reason why the HDL-based model correlates well with practice is that it can incorporate the actual shape and size of various components into the micro-generator model by using analytical equations. Here the non-linear dependence of the micro-generator’s output voltage on the input displacement described in Section 2.3 can be accurately captured by the HDL model. Simulation results of the equivalent circuit model and HDL model are compared with the experimental measurement in Fig. 2.11. As can be seen from the waveforms, when excited by a sine wave stimulus, the equivalent circuit model still generates sine wave output. But the HDL model can capture the situations when the coil and magnets are moving apart, which is what happens in practice and leads to non-sine wave output.



(a)



(b)

Fig. 2.10 Experimental measurement set-up: (a) micro-generator sitting on a vibration generator and (b) Labview software collecting the data

Although the simulation results of the proposed HDL models are very close to the experimental measurements, there are still notable differences between them in both Figs. 2.9 and 2.11. The reasons may be found by examining the practical conditions during experiments. In Fig. 2.9, the charging waveforms do not start from 0 V because in practical measurements the capacitors all had a bit of initial charge and adjustments on the timing have been made to the simulation waveforms so that all the curves start at the same voltage (about 0.6 V), which may lead to the difference. In Fig. 2.11, the difference between the simulation waveform and experimental measurement may be generated by the interference that was brought in by the oscilloscope's probes.

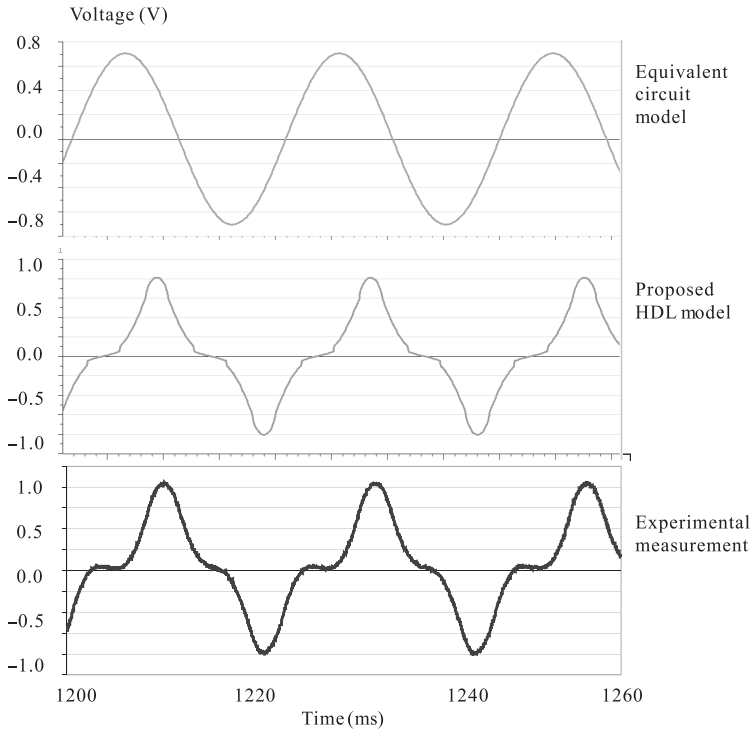


Fig. 2.11 Non-linear output from micro-generator correctly reflected by proposed model

2.4 Automatic Structure Configuration Based on HDL Model Library

From the last section, a small HDL model library of energy harvester components has been built. It contains two types of micro-generator, each of which can be configured with different coils (wire diameter of 12/16/25 μm) and two types of voltage multipliers that have three to six stages. The voltage transformer has not been included because it cannot be made and tested with available resources. But the simulation-based optimisation of energy harvester with voltage transformer has been performed and will be discussed in Section 2.5.2. The configuration target has been set to find the set of components that can charge the 0.047 F supercapacitor to 2 V in shortest time. These values were chosen because there has been reported energy harvester systems that use 0.047 F storage capacitor and 2 V working voltage [17].

Simulations of every available energy harvester configuration were carried out simultaneously and a process has been developed to automatically track the best model. SystemVision VHDL-AMS simulator [5] has been used as the single software platform. The outcome design is listed in Table 2.2.

Table 2.2 Parameters of the configuration result

Micro-generator	Type II
Wire diameter	25 μm
Voltage booster	Three-stage Dickson VM (Fig. 2.6e)

Not surprisingly, the micro-generator II has been chosen because it is bigger and stores more kinetic energy. However, it is quite interesting that the coil with the largest wire diameter, which leads to fewest number of turns, and the VM with fewest stages have been chosen. To further investigate on this result, more simulations have been done and an important trade-off between the electromagnetic micro-generator and the VM voltage booster has been found.

Figure 2.12 shows the charging waveforms of type I micro-generator connected to the same five-stage VM but configured with different coils. At the beginning, the energy harvester with 25 μm wire diameter charges the quickest and the 12 μm configuration charges the slowest while the 16 μm one is in between. But the 25 μm configuration also saturates quickly and reaches the 2 V mark slower than the 16 μm energy harvester. Due to simulation time limitation, the figure does not show how the other two waveforms end. But it could be foreseen that the 16 μm configuration will also saturate at some point while the 12 μm one reaches highest voltage.

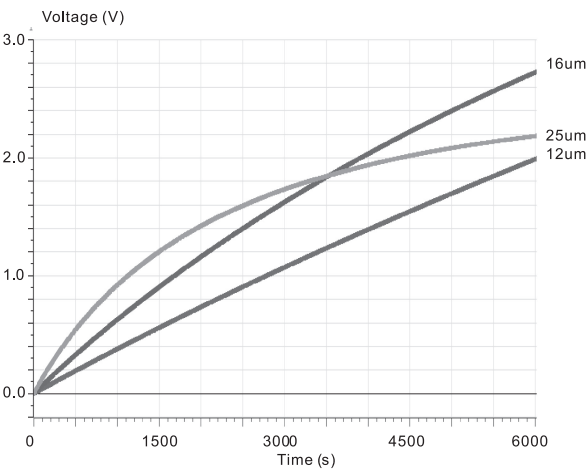


Fig. 2.12 Simulation of type I micro-generator with different coils

Similar results have been obtained from the voltage booster end. Figure 2.13 shows the charging waveforms of type II micro-generator with 25 μm coil connecting with three-, four- and five-stage Dickson VMs. It can be seen that the energy harvester with three-stage VM charges the supercapacitor to 2 V first and the one with five-stage VM can reach the highest voltage.

From the simulation results it can be concluded that in an energy harvester design that combines electromagnetic micro-generator and voltage multiplier, the fewer

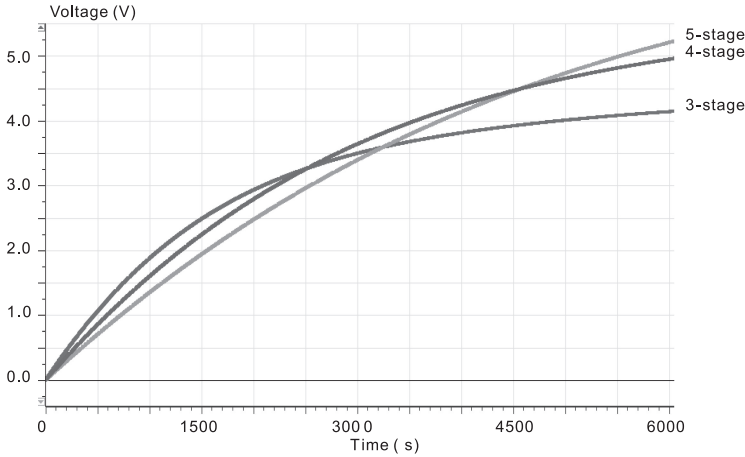


Fig. 2.13 Simulation of type II micro-generator with different VMs

number of turns in the coil and the fewer VM stages, the higher initial charging rate the energy harvester can get but the lower voltage it can finally reach. Therefore, although the micro-generator with more coil turns can generate more power and VMs with more stages can boost the voltage higher, under certain circumstances the optimisation of subsystems in isolation does not lead to a globally optimised design. It proves that when combining different components of an energy harvester, the gain at one part may come at the price of efficiency loss elsewhere, rendering the energy harvester much less efficient than expected. This information is very useful for the development of future, more complicated systems and model libraries.

2.5 Performance Optimisation

The close mechanical–electrical interaction (micro-generator and voltage booster) that takes place in energy harvesters often leads to significant performance loss when the various parts of the energy harvesters are combined. Here the loss expressed in terms of energy harvesting efficiency

$$\eta_{\text{Loss}} = \frac{E_{\text{Harvested}} - E_{\text{Delivered}}}{E_{\text{Harvested}}} \quad (2.13)$$

In the proposed design flow, the generated energy harvester design should be parameterised such that automated performance optimisation will be able to further improve the energy harvester efficiency by employing suitable optimisation algorithms. The parameters used for the optimisation are from both the micro-generator and the voltage booster. The optimisation object is to increase the charging rate of the supercapacitor.

2.5.1 Exhaustive Search

The micro-generator parameters that can be optimised are related to the coil size, i.e. the thickness (t) and the outer radius (R), because other components such as the magnets and cantilever determine the resonant frequency of the micro-generator and thus should be based on application requirements. The circuit parameters of voltage booster are the capacitor values of each VM stage. The entire energy harvester is optimised as an integrated model. The searching space of parameters has been given in Table 2.3

Table 2.3 Optimisation searching space	Coil thickness (mm)	1.0–1.3
	Coil radius (mm)	2.0–2.45
	Capacitor values (μF)	47/100/150

The optimisation is based on the concurrent simulations of design instances from uniform sampling of the search space and tracking the best result (Fig. 2.14). This is relatively simple and straightforward because after the automatic structure configuration the search space is quite small and the VM capacitors can only have discrete values. However, other optimisation algorithms may also be employed and in Section 2.5.2 a VHDL-AMS-based genetic optimisation has been successfully applied to the integrated optimisation of energy harvester systems.

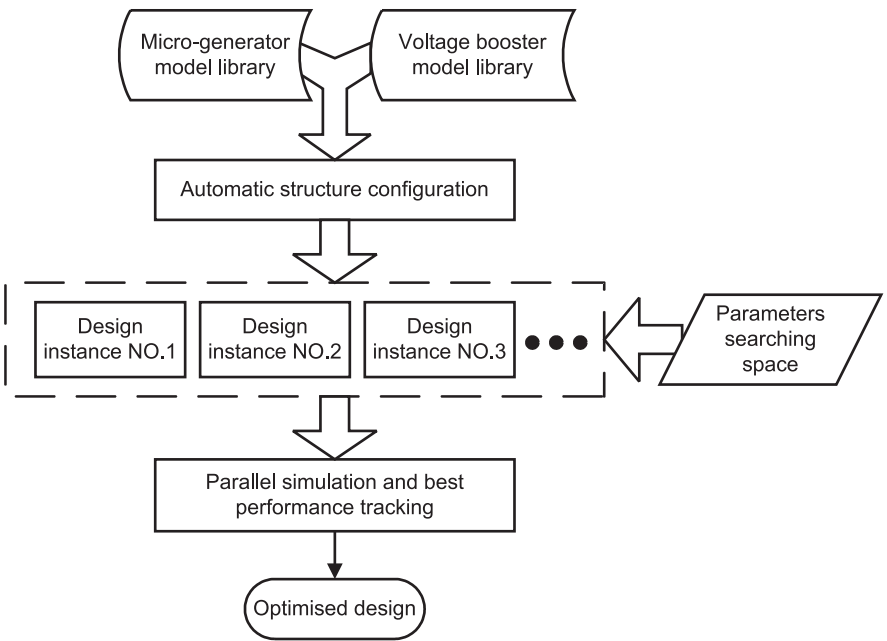


Fig. 2.14 Implementation of the proposed energy harvester design flow in VHDL-AMS

To validate the effectiveness of the proposed approach to improve energy harvesting efficiency, the following simulations and experimental measurements have been carried out.

2.5.1.1 Original Design

This combines type II micro-generator with a five-stage Dickson VM. The used VM has been reported in literature as optimal configuration [18]. However, in the original design these two parts are optimised separately, which is quite common in existing energy harvester design approach. Parameters of original design are listed in Table 2.4.

Table 2.4 Parameters of original energy harvester

<i>Micro-generator</i>	
Wire diameter (μm)	16
Coil thickness (mm)	1.3
Coil radius (mm)	2.45
<i>Voltage booster</i>	
VM configuration	five-stage Dickson
Capacitor values (C1–C5, μF)	47,150,150,47,150

2.5.1.2 Optimised Design

This has been obtained using the proposed design flow (Fig. 2.14). Table 2.5 gives the new micro-generator and voltage booster parameters.

Table 2.5 Parameters of optimised energy harvester

<i>Micro-generator</i>	
Wire diameter (μm)	25
Coil thickness (mm)	1.3
Coil radius (mm)	2.0
<i>Voltage booster</i>	
VM configuration	Three-stage Dickson
Capacitor values (C1–C3, μF)	100,100,47

The impact of these values on improving the energy harvester performance has been validated in both simulation and experimental measurements. According to the optimisation result, a new coil has been ordered from Recoil Ltd, UK [12], and replaced the original one for testing (see Fig. 2.15).

Simulation and experimental waveforms of the original and optimised design are shown in Fig. 2.16. The impact of using the supercapacitor model in Fig. 2.8 instead of an ideal capacitor has also been investigated. As can be seen from the figure, there is good correlation between the simulation and experimental waveforms in both of the energy harvester designs, which validates the effectiveness and accuracy of the

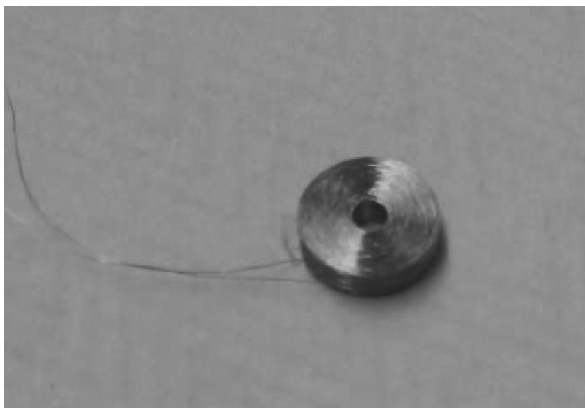


Fig. 2.15 New coil according to optimisation result ($R = 2.0$ mm, $r = 0.5$ mm, $t = 1.3$ mm, $d = 25$ μ m)

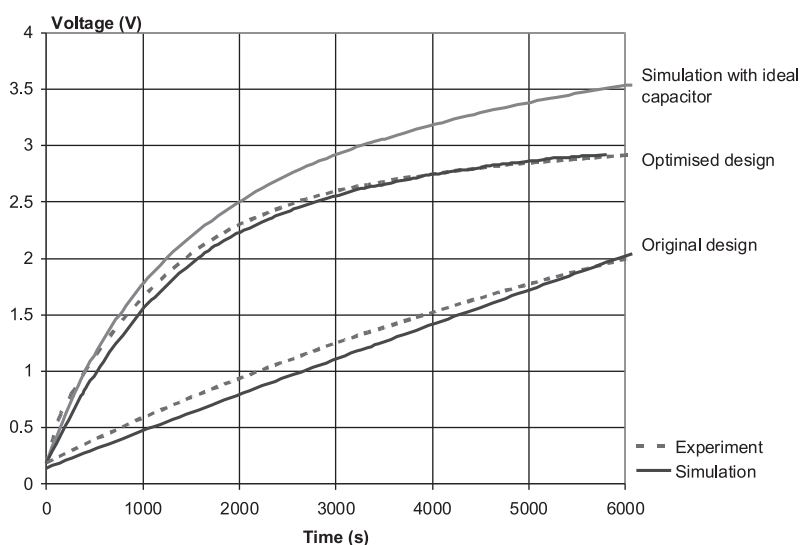


Fig. 2.16 Simulation and experimental waveforms of original and optimised energy harvesters

proposed design flow. The energy harvester from original design can charge the supercapacitor to 2 V in 6000 s while the optimised design only uses 1500 s, which represents a 75% improvement.

2.5.2 Genetic Optimisation

This section demonstrates another possible optimisation method to improve the energy harvester efficiency. Figure 2.17 shows that in the proposed approach, not

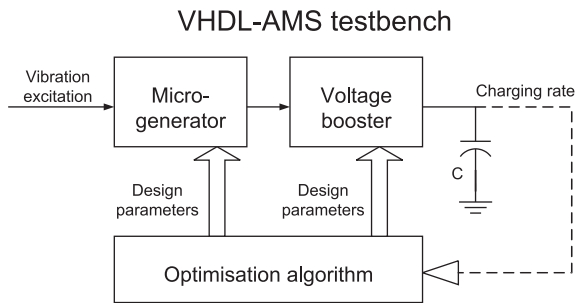


Fig. 2.17 Integrated performance optimisation in VHDL-AMS testbench

only the energy harvester model but also the optimisation algorithm is implemented in a single VHDL-AMS testbench. The parameters used for the optimisation are from both the micro-generator and the voltage booster. The optimisation object is to increase the charging rate of the supercapacitor. The optimisation algorithm generates design parameters to the model and obtains the charging rate through simulation. The optimisation loop runs continuously until the design parameters reach an optimum.

A supercapacitor of 0.22 F has been used in the performance optimisation experiment. The micro-generator parameters that can be optimised are the number of coil turns (N), the internal resistance (R_c) and the outer radius (R). The voltage booster circuit is the voltage transformer described in Section 2.3.2.2 (Fig. 2.7). The parameters are the number of turns and the resistance of primary and secondary windings. For proof of concept, we employed a genetic algorithm (GA) [7] to optimise the energy harvester with a voltage transformer booster. The implemented GA has a population size of 100 chromosomes. Each chromosome has seven parameters (three from the micro-generator and four from the voltage booster). The crossover and mutation rate are 0.8 and 0.02, respectively. Other optimisation algorithms may also be applied based on the proposed integrated model. The “unoptimised” model parameters are given in Table 2.6.

Applying the proposed modelling and performance optimisation, Table 2.7 gives the new micro-generator and voltage booster parameters which are referred to as “optimised” design. The impact of these values on improving the charging of the supercapacitor is shown in Fig. 2.18. As can be seen from the simulation results,

Table 2.6 Parameters of unoptimised energy harvester

<i>Micro-generator</i>		
<hr/>		
Outer radius of coil (R)		1.2 mm
Coil turns (N)		2300
Internal resistance (R_c)		1600 Ω
<hr/>		
<i>Voltage transformer</i>		
<hr/>		
	Resistance(Ω)	No. of turns
Primary winding	400	2000
Secondary winding	1000	5000
<hr/>		

Table 2.7 Parameters of GA-optimised energy harvester

<i>Micro-generator</i>		
Outer radius of coil (R)		1.1 mm
Coil turns (N)		2100
Internal resistance (R_c)		1400 Ω
<i>Voltage transformer</i>		
	Resistance (Ω)	No. of turns
Primary winding	340	1900
Secondary winding	690	3800

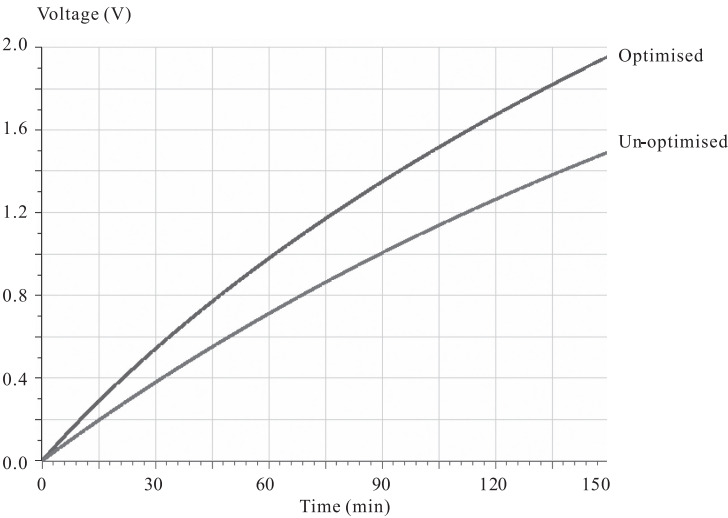


Fig. 2.18 Simulation waveforms of supercapacitor charging by different energy harvester models

in 150 min the unoptimised energy harvester charges the supercapacitor to 1.5 V and the optimised energy harvester reaches 1.95 V, which represents a 30% improvement.

Performance of the developed GA has been further investigated by comparing the power transfer efficiency before and after optimisation. The maximum average power that can be delivered to the electrical domain is about 144 μW , calculated from Eq. (2.10). Table 2.8 lists the average electrical power output from the micro-generator and the voltage transformer. It can be seen that the optimisation improves the efficiency of both the micro-generator and voltage booster, which validates the effectiveness of the developed genetic optimisation.

Table 2.8 Energy harvester power efficiency

	Generated power (μW)	Generator efficiency (%)	Delivered power (μW)	Transformer efficiency (%)	Overall efficiency (%)
Pre-optimisation	26.875	18.66	15.750	58.60	10.94
Post-optimisation	29.250	20.31	19.625	67.09	13.63

2.6 Concluding Remarks

This chapter presents an automated energy harvester design flow that can generate optimised configuration from an existing HDL model library as well as carry out performance optimisation through the employment of a single software platform. The effectiveness of the proposed design flow has been demonstrated by automatic configuration, optimisation and experimental validation of an energy harvester powered by an electromagnetic vibration-based micro-generator. It has been shown that the existing energy harvester design approaches are inadequate because there is a trade-off between different energy harvester components and the optimisation of subsystems in isolation does not lead to a globally optimal design. A new energy harvester has been manufactured according to the outcome from the proposed design flow and experimental measurements of the new device have validated the optimisation results. It has been shown that the outcome from the design flow (configuration and optimisation) can achieve a 75% improvement in the supercapacitor charge rate and the integrated performance optimisation alone may achieve a 30% improvement.

References

1. Amirtharajah R, Wenck J, Collier J, Siebert J, Zhou B (24–28 July 2006) Circuits for energy harvesting sensor signal processing. In: Design Automation Conference, 2006 43rd ACM/IEEE, Anaheim, CA 639–644
2. Beeby S, Torah R, Tudor M, Glynne-Jones P, O'Donnell T, Saha C, Roy S (2007) A micro electromagnetic generator for vibration energy harvesting. *J. Micromech. Microeng.* 17(7):1257–1265
3. Beeby SP, Tudor MJ, White NM (2006) Energy harvesting vibration sources for microsystems applications. *Meas. Sci. Technol.* 17(12):R175–R195
4. von Buren T, Mitcheson P, Green T, Yeatman E, Holmes A, Troster G (2006) Optimization of inertial micropower generators for human walking motion. *Sens. J. IEEE* 6(1):28–38
5. Corporation MG (July 2004) SystemVision User's Manual. Version 3.2, Release 2004.3
6. El-Hami M, Glynne-Jones P, White N, Hill M, Beeby S, James E, Brown A, Ross J (2004) Design and fabrication of a new vibration-based electromechanical power generator. *Sens. Actuators A: Phys.* 92(1–3):335–342
7. Mitchell M (1996) An Introduction to genetic algorithms. MIT Press, Cambridge, MA
8. Mitcheson P, Green T, Yeatman E, Holmes A (2004) Architectures for vibration-driven micropower generators. *J. Microelectromech. Syst.* 13(3):429–440
9. Mitcheson P, Miao P, Stark B, Yeatman E, Holmes A, Green T (2004) MEMS electrostatic micropower generator for low frequency operation. *Sens. Actuators A: Phys.* 115(2–3):523–529
10. Nelms R, Cahela D, Newsom R, Tatarchuk B (14–18 March 1999) A comparison of two equivalent circuits for double-layer capacitors. In: Applied Power Electronics Conference and Exposition, 1999, vol. 2. APEC '99. Fourteenth Annual, Dallas, TX 692–698
11. Ottman G, Hofmann H, Bhatt A, Lesieutre G (2002) Adaptive piezoelectric energy harvesting circuit for wireless remote power supply. *Power Electron. IEEE Trans.* 17(5):669–676
12. Recoil Ltd, UK (Sept. 2008) <http://www.recoiltd.com/index.htm>
13. Saha CR, O'Donnell T, Loder H, Beeby S, Tudor J (2006) Optimization of and electromagnetic energy harvesting device. *Magnetics, IEEE Trans.* 42(10):3509–3511

14. Shao H, Tsui CY, Ki WH (21–24 May 2006) A charge based computation system and control strategy for energy harvesting applications. In: Circuits and Systems, 2006. ISCAS 2006. Proceedings. 2006 IEEE International Symposium, Island of Kos, Greece 2933–2936
15. Siebert J, Collier J, Amirtharajah R (8–10 Aug. 2005) Self-timed circuits for energy harvesting AC power supplies. In: Low Power Electronics and Design, 2005. ISLPED '05. Proceedings of the 2005 International Symposium, San Diego, CA, 315–318
16. Torah R, Beeby SP, Tudor MJ, O'Donnell T, Roy S (2006) Development of a cantilever beam generator employing vibration energy harvesting. In: Proceedings of the 6th Int. Workshop on Micro and Nanotechnology for Power Generation and Energy Conversion Applications, Berkeley, CA 181–184
17. Torah R, Glynne-Jones P, Tudor J, O'Donnell T, Roy S, Beeby S (2008) Self-powered autonomous wireless sensor node using vibration energy harvesting. *Meas. Sci. Technol.* 19(12):ISSN 1361–6501
18. Torah R, Tudor M, Patel K, Garcia I, Beeby S (28–31 Oct. 2007) Autonomous low power microsystem powered by vibration energy harvesting. In: Sensors, 2007 IEEE, Atlanta, GA, 264–267
19. Tsui CY, Shao H, Ki WH, Su F (24–27 Jan. 2006) Ultra-low voltage power management circuit and computation methodology for energy harvesting applications. In: Design Automation, 2006. Asia and South Pacific Conference, Yokohama, Japan 96–97
20. Wang A, Chandrakasan A (2005) A 180-mV subthreshold fet processor using a minimum energy design methodology. *IEEE J. Solid State Circuits* 40(1):310–319
21. Williams C, Shearwood C, Harradine M, Mellor P, Birch T, Yates R (2001) Development of an electromagnetic micro-generator. *Circuits, Dev. Syst. IEE Proc.* 148(6):337–342
22. Yan H, Macias Montero J, Akhnoukh A, de Vreede L, Burghartz J (17–18 Nov. 2005) An integration scheme for RF power harvesting. In: Proceedings STW Annual Workshop on Semiconductor Advances for Future Electronics and Sensors, Veldhoven, The Netherlands 64–66

Energy Harvesting Systems
Principles, Modeling and Applications
Każmierski, T.J.; Beeby, S. (Eds.)
2011, XI, 163 p., Hardcover
ISBN: 978-1-4419-7565-2